Pergamon

PII S0016-7037(00)00605-0

In situ investigation of galena dissolution in oxygen saturated solution: Evolution of surface features and kinetic rate

GIOVANNI DE GIUDICI*,† and PIERPAOLO ZUDDAS

Laboratoire de Géochimie des Eaux, CNRS 7047-Institut de Physique du Globe de Paris and Université Paris 7, 2, Place Jussieu, case 7052,
F75251 Paris Cedex 05, France

Abstract—In this work, an original Atomic Force Microscopy (AFM) investigation was carried out combining in situ microtopography measurements with solution chemistry. The dissolution of galena (PbS) surface in acidic (HCl, pH = 1) and oxygen saturated solution was investigated in an AFM liquid cell at room temperature over 45 h. In this apparatus, solution circulates into the flow-through reactor at high-flow rate and is periodically sampled for chemical analysis. In the first hours of microtopography measurement square etch pits delimited by steps of minimal depth of 1 nm nucleate and growth attaining a maximal depth of 80 nm. After this short stage, surface features evolve by formation of widespread protrusions 1 to 3 nm high and homogeneously distributed, while nucleation and growth of new etch pits is inhibited, and large rough terraces delimited by macrosteps 50 to 100 nm high are formed by dissolution. The solution interacting with galena surface is strongly undersaturated with respect to both galena and anglesite (PbSO$_4$), namely solution saturation state for these minerals decreases during the experiment by more than two order of magnitude, and dissolution rate was then derived from lead concentration in solution. During the duration of the experiment, dissolution rates decrease by more than one order of magnitude attaining a final value of $4.5 \pm 0.5 \times 10^{-8}$ mol m^{-2} sec^{-1}. Other dissolution experiments performed using different mineral grains confirmed the reproducibility of the galena surface evolution process. However, protrusion observed at lower hydrogen ion activity (pH = 3) showed a rounded shape. From thermodynamic and XPS data in the literature, we predicted that nanometric protrusions are composed of native sulphur, an intermediate and slowly dissolving phase that, in turn, react with oxygen to dissolve and migrate towards bulk solution in a more oxidised state (eg. as SO_4^{2-}, $S_2O_3^{2-}$, etc.).

We interpreted that the protrusion dissolution reaction represents the step limiting the rate of the overall dissolution reaction, and the evolution of the rate regime is a transitory stage due to the continuous increase in the thickness of the altered layer that coats the surface. Finally, this nanoscale detailed description of galena dissolution process is relevant in terms of both reaction mechanisms and computational modelling of metal sulphide oxidation processes. *Copyright © 2001 Elsevier Science Ltd*

1. INTRODUCTION

Mechanisms of sulphide mineral dissolution are central to several Earth surface processes such as acid mine drainage, contaminant desorption and low-enthalpy water-rock interaction (Singer and Stumm, 1970; Wieland et al., 1988; Reeder, 1991; Nesbitt and Muir, 1994; Nesbitt et al., 1995). Galena is one of the main minerals controlling the mobility of lead in these aqueous environments with, very often, low pH and oxygen saturated fluid conditions. A significant number of investigations produced a reasonable understanding of the chemical forms of the reaction products. X-ray photoelectron spectroscopy (XPS), indicate that in acidic and oxidative solutions lead oxide, lead hydroxide and sulphate, can be found on the reacted surface of galena (Fornasiero et al., 1994; Kim et al., 1995). On the other hand, investigations based on the solution chemistry suggest that galena dissolution reaction is congruent with respect to the Pb/ΣS pair and slightly pH-dependent (Hsieh and Huang, 1989). The advent of scanning probe microscopes [e.g., atomic force microscopy (AFM) and scanning tunnelling microscopy (STM)] has opened a new

discussion on where and when oxidation products form and the nature of their physical form. In air exposed galena surfaces, Eggleston and Hochella, (1991) and Eggleston (1996) found evidence for oxidation of S sites by atomic or molecular oxygen while Kim et al. (1994) proved that oxidation proceeds faster for natural galena than synthetic impurity-free specimens. They also observed that oxidation products cover indiscriminately edges and terraces in natural specimens while are preferentially located on edges on synthetic free-impurity specimens. Investigating the dissolution of (001) surface in acidic and oxygen depleted aqueous conditions by an electrochemical scanning tunnelling microscope (ECSTM), (Higgins and Hamers, 1995; 1996) found that dissolution produces etch pits delimited by elementary steps preferentially oriented along [110] crystallographic directions while sulphur atomic islands can be formed when the applied electrochemical potential corresponds to the theoretical value of sulphur formation. Besides the properties of surface atomic structure, the character of this mineral during interaction with water should depend also on chemisorbed oxygen at the surface as proposed by Tossel and Vaughan (1987 and references therein) because it should produce the modification of both surface conductivity and surface reaction sites. Such a dependence of galena surface behaviour upon reaction conditions is confirmed also by elec-

---

* Author to whom correspondence should be addressed.
† *Present address:* Dip. Scienze della Terra, Università di Cagliari, Via Trentino 51-09100 Cagliari, Italy (gbgiudic@unica.it).

tokinetic measurements of pH isoelectric point (pH$_{i.e.p.}$) of galena and other metal sulphide surfaces. In fact, these measurements indicate values of pH$_{i.e.p.}$ in the range between pH of 0.6 and 3.3 mainly dependent upon the properties of sulphur atom (Bebie et al., 1998), but pH$_{i.e.p.}$ can be shifted by several units of pH by a change in surface charge of oxidising sulphide surface like pyrite (Fornasiero et al., 1991).

The intent of this work is to measure in situ both surface microtopography and chemistry of the interacting solution. The fundamental questions that we would answer by this two-days long investigation in the flow-through reactor of AFM are how galena surface behaves during interaction with oxygen-saturated solution having constant solution pH, and does interacting solution attain a chemical steady state? In the literature, there are few works that present molar and microtopographic in situ measurements carried out together on the same sample. In future, this simple experimental apparatus can be used to investigate the reactivity of other minerals in different experimental conditions (namely temperature, flow rate, controlled atmosphere, etc.), and should allow quantitative assessing of kinetic and scale laws that relate laboratory and field-scale experiments.

2. EXPERIMENTAL METHODS

We selected a large specimen of galena from Iglesiente mine, (Italy). X-ray fluorescence analysis of freshly cleaved surfaces showed that this natural specimen has Zn, Fe and Cu trace impurities of 0.2, 0.1 and 0.1% (in atoms) respectively. A freshly cleaved surface obtained upon cleaving a cubic grain of galena was imaged by AFM in oxygen saturated HCl-H$_2$O solution (pH values of 1 and 3).

Traces of transition metals, as commonly found in natural samples, can influence the reactivity of semiconductor surfaces as PbS by increasing their conductivity (Tossel and Vaughan, 1987; Xu and Schoonen, 1996). Furthermore, impurities adsorbed at the reacting surface are often considered to influence step kinetics and, then, surface features of many minerals observed by AFM (see for example Land et al., 1999). However, in our oxygen saturated solutions, transition metals were much lower concentrated (<10^{-8} mol/L) than dissolved oxygen and their effect was then assumed to be negligible in the overall process of galena dissolution.

AFM investigation was performed using a Molecular Imaging microscope equipped with Digital Instruments software, a 7.5 μm × 7.5 μm scanner and a teflon liquid cell commercially available. In the Molecular Imaging microscope, the stage holding sample and liquid cell stays below the scanners and was lodged in a small chamber to avoid acoustical noise and dust contamination from the room atmosphere. All the images were taken in constant force mode while displaying both height and deflection signal of the cantilever, and the adopted silicon tips (nominal force constant of 0.2 N/m) allowed the tip-surface force in liquid lower than 1 nN. To prevent perturbation during the two days of interaction the tip scanned the surface only during the time of image collection. All the images have been collected at the scan rate value of 4 Hz and with 256 lines per scan, i.e., the elapsed time from the top to the bottom of each image was 1 min. To exclude the possibility of dirty tip formation, we rotated scan angle during image collection, and imaged a surface standard of mica at the end of the experiment always finding the expected features. To obtain the condition of solution saturation in oxygen, solution reservoir and liquid cell were open to the room atmosphere via air-permeable filters; thus, for the room temperature of 20 ± 2°C, experimental oxygen partial pressure was about 2 × 10^4 Pa. A peristaltic pump provided a continuous renewal of interacting solution with a controlled flow rate, Q, of 270 μl/min. In our experiment, the teflon liquid cell was not completely filled and the volume of solution in the cell was 100 μL, then the complete renewal of solution was done in ≈20 s.

Roughness analysis was performed by DI software on height mode images without applying planefit nor flatten DI correction during image

analysis. Note that, when atoms are not laterally resolved in the image, roughness measurements by AFM give us information about nanometric details in the three dimensions but not about the amount of atomic vacancies present at the surface. However, although the absolute roughness value given by AFM can be underestimated, the relative difference measured for a sequence of images give us a valid estimation of roughness evolution during the dissolution reaction of galena.

Initial solution did not contain lead nor sulphur dissolved, and dissolution rate of galena, R_{Pb}, (mol m^{-2} sec^{-1}) was evaluated by:

$$R_{Pb} = (Pb^{2+}_{output}) \times \frac{Q}{A} \tag{1}$$

where Pb^{2+}_{output} is the analytical concentration of lead in solution and A, is the amount of total surface area in contact with solution. A, was estimated as geometric area of the grain (a perfect parallelepiped of 1.4 × 1.8 × 2.9 mm) and means 2 ± 0.4 × 10^{-5} m^2. This value was confirmed by AFM roughness estimations made by DI software. Note that data reported in this work were carried out in a single experiment, and the Q/A ratio was constant during the reaction.

The input solution was prepared adding HCl to Milli-Q deionised water (under room atmosphere) to reach the desired pH value. Solution pH value was measured before and after interaction and did not change over the entire experiment. The calibration of pH electrode was made using NIST reference standards. During the reaction, 1–2 mL of solution were periodically collected from the output line, immediately filtered through 0.45 μm cellulose nitrate filters and later analysed for total dissolved lead by Graphite Furnace Atomic Absorption Spectroscopy (HITACHI, equipped with Zeemann effect) with a precision (3σ) of 5%.

3. RESULTS AND DISCUSSION

3.1. Kinetic Rate

The kinetics of galena dissolution in acidic oxidative conditions have been classically described by an initial surface protonation followed by adsorption of O$_2$ molecules and oxidation of sulphide to sulphate at the liquid-solid interface or in solution (Hsieh and Huang, 1989) resulting in the release of lead to solution. At a given constant pH, the overall dissolution reaction can be schematically represented by a simplified mass balance equation:

$$PbS + nO_2 \rightarrow Pb^{2+} + (S_{tot})^{2-} \tag{2}$$
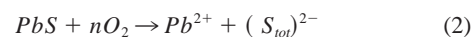
where $(S_{tot})^{2-}$ represents the total dissolved sulphur species in solution.

Total dissolved lead was measured in our experimental solutions, while total dissolved sulphur was not detectable by our routine analysis (see Appendix). In our acidic oxidative conditions galena dissolves in far from equilibrium conditions and the stable phase of sulphur that could eventually precipitate from solution is anglesite (PbSO$_4$). We can estimate the solution saturation state with respect to both galena and anglesite assuming that galena dissolves congruently (Hsieh and Huang 1989), and that dissolved H$_2$S is about 10% of total dissolved sulphur and sulphate is 90%. In such a way, we found that solution circulating in the liquid cell was strongly undersaturated with respect to both primary

$$\left(\Omega_{galena} = \frac{[Pb^{2+}] \times [HS^-]}{[H^+] \times K_s} < 2 \times 10^{-4}, K_s = 10^{-12.75 \pm 0.05} \right)$$

and secondary phase

$$\left(\Omega_{anglesite} = \frac{[Pb^{2+}] \times [SO_4^{2-}]}{K_s} < 2 \times 10^{-3}, K_s = 10^{-7.79 \pm 0.02} \right),$$
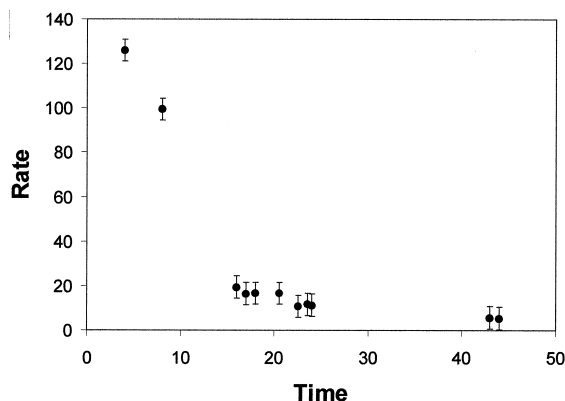
Fig. 1. Dissolution rate (10^{-8} mol m^{-2} sec^{-1}) of galena in acidic oxidative solution (pH = 1) was a function of time (h) estimated by the flow through system of the AFM liquid cell.

as reported in the Appendix I. At the molar scale of the overall reaction, dissolved lead is thus mainly related to the dissolution of galena and dissolution rate was estimated by the amount of lead released to solution (Eqn. 1), and plotted as a function of time (Fig. 1). The rate decreases rapidly (one order of magnitude) in the first stage and clearly more slowly in last 30 h of reaction. Since in our flow-through reactor initial solution has constant composition and is renewed at constant rate, such a variation of the rate regime exclusively results from a change in the state of the reacting surface. On the other hand, estimating the value of ΔG with respect to the dissolution of galena (Appendix I), we surprisingly found that the highest dissolution rates correspond to $\Delta G \approx -21$ KJ mol^{-1}, while the lowest rates correspond to the value of about -35 KJ mol^{-1}. Dissolution rates are then inversely related to the estimated ΔG in contrast with the theoretical relationship between reaction rate and ΔG (see for example Lasaga, 1998). Thereby, macroscopic thermodynamic driving force is perhaps governed by microscopic phases other than PbS forming at oxidising galena surface.

On the other hand, it must be noted that our experiment has been carried out at the condition of constant solution pH, thus, measured dissolution rates indicate a mechanistic dependence upon hydrogen activity not constant during the investigation. Such an evolution of the kinetic regime can be explained by an evolution in the chemical speciation at the dissolving surface and/or a change in the structure of the interface able to influence the diffusion of the species participating to the reaction.

3.2. Evolution of the Surface Microtopography

Our initial surface (Fig. 2a) is characterised by square cavities $100-500$ nm large, a step of 5 nm as well some powders made of galena debris. After 2 min of interaction with HCl solutions (Fig. 2b), all the powders previously observed disappear while new square pits having an average horizontal size of 30 nm and depth of 1 nm, are formed by dissolution. Pits generate in domains initially flat while previously formed cavities growth either conserving a square shape or coalescing in larger pits. Figures 1c,d, taken after 25 and 38 min respectively, show that the pit density increases and pit size growths with an estimated mean velocity of 15 and 1.5 nm/min in the horizontal and vertical directions respectively (Appendix II).

After 17 h of interaction etch pits become $50-80$ nm deep (Fig. 1e). However, a zoom (Fig. 2f) clearly shows that the surface is characterised by a microroughness made of pyramidal protrusions $1-3$ nm high and homogeneously distributed. After 40 h of interaction (Fig. 2g), terraces are delimited by macrosteps 50 to 100 nm high and surface is characterised by microroughness. At this stage the pits previously formed are redissolved, indicating that dissolution is ever active and a thickness of several tens of nm has been removed after the appearance of protrusions.

Our nanometric estimations do not provide evidence of elementary steps at the surface nor at the walls of the pits. In fact, the minimal vertical dimension that was measured is 1 nm while the theoretical distance between two neighbouring atoms of Pb and S in the fcc lattice is 2.97 A. However elementary steps should be present on these sloped pit walls but terraces are not wide enough to be individually resolved. By contrast, in oxygen-free acidic and oxidative conditions, Higgins and Hamers (1996) found that dissolution produces large terraces and proceeds via the retreat of steps height of 3.2 ± 0.4 A (or a multiple of the Pb-S interatomic distance) and oriented along [110] crystallographic direction. We also found that in our experimental conditions, protrusions cover the entire observed surface while they are rare and isolated in the oxygen-free oxidative conditions of Higgins and Hamers (1995) and Higgins and Hamers (1996). This difference in the surface microtopography suggests that galena surface behaves differently as a function of the oxidative conditions of the solution, and confirms that chemisorbed oxygen is an agent able to modify the conductivity of galena surface thus changing its reactivity (Tossel and Vaughan, 1987).

The significant evolution of the surface morphology can be represented by the variation of the roughness coefficient. This parameter, defined by the ratio between mineral surface area at a given time and initial surface area (Jaycock and Parfitt, 1981; Anbeek, 1992) represents, in fact, the 'degree of order' of the surface during the reaction of dissolution (Lasaga, 1998). Estimating the surface roughness coefficient by the D.I. software, we found that the increase of the roughness in the 45 h of interaction corresponds to a few percent, during the stage of strong decrease in dissolution rates surface roughness is constant, and roughness increase is mainly produced in the period between the collection of Figure 2e,g. Note that dissolution rates normalised by constant surface area decrease by more than one order of magnitude. Thereby, only a huge increase in surface area during dissolution reaction could balance that decrease and make constant the value of dissolution rate, but this is in contrast with AFM data. Thus, the hypothesis of constancy of total surface area assumed in the estimation of dissolution rate at the molar scale (Eqn. 1) is confirmed.

The kinetic parameter that should be used in kinetic rate equation is reactive area, and this can be derived from AFM images. However, our AFM data do not allow us the quantitative assessment of reactive area over the entire investigation period, but clearly suggest that reactive area changes when pyramidal protrusions appear. In other words, the initial reactive area is concentrated on fast reacting etch pits area whereas protrusion reactive area extends to the entire surface. This change in reactive area reflects the evolution in the kinetic regime observed at the molar scale.
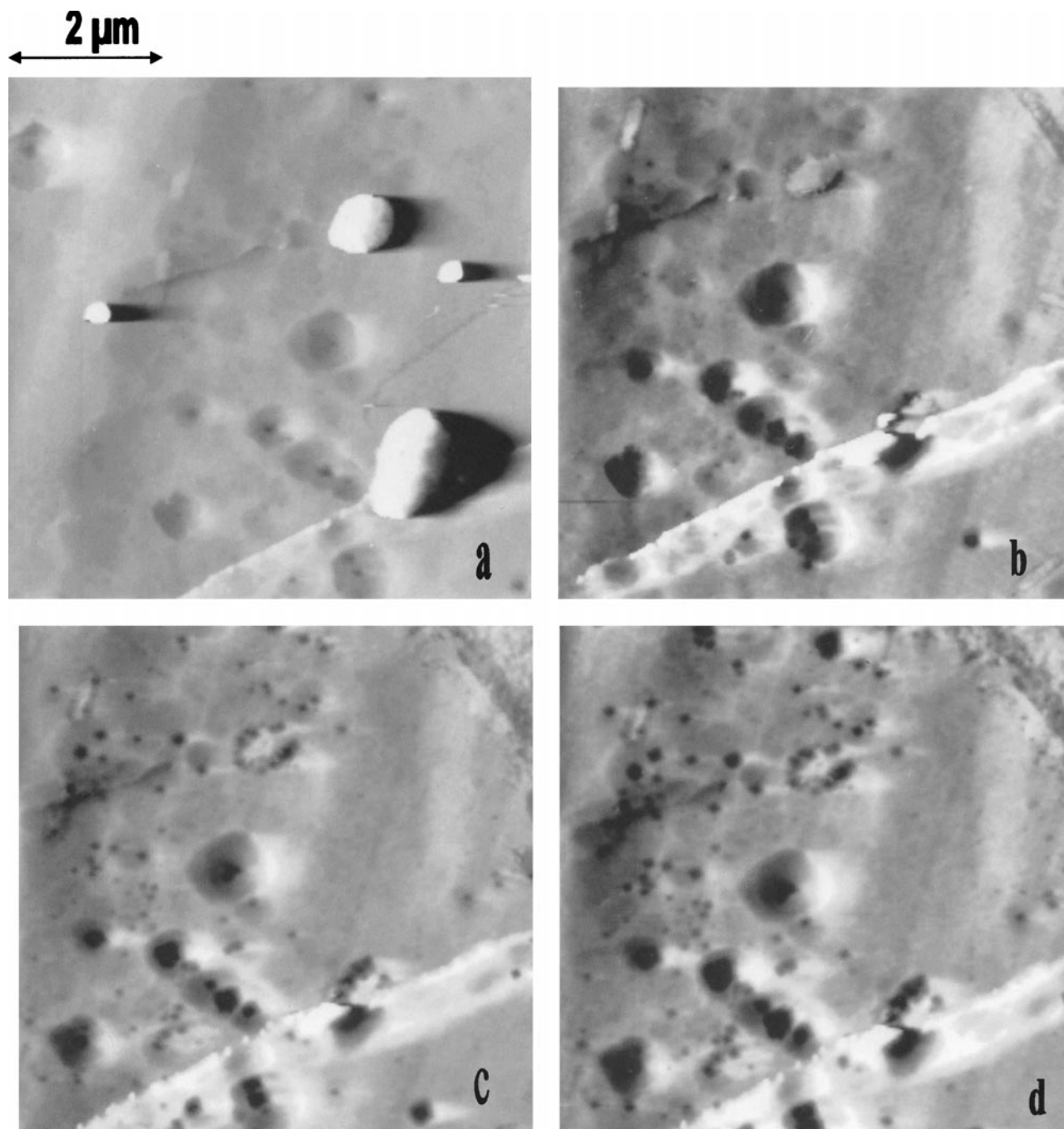
Fig. 2. AFM 7×7 μm horizontal scale images of PbS surface during dissolution in acidic and oxygen saturated solution (f was collected in height mode, the other images in deflection mode). Acquisition time from the top to the bottom of the image is 1 min. An artificial light from the left of the image makes the left sides of the pit walls shaded. (a) is the (001) freshly cleaved surface, covered by some galena debris. (b) to (g) The surface interacting with pH = 1 solution (HCl) as a function of time. (b) The surface after 2 min of interaction, (c) after 28 min, and (d) after 38 min. In this first stage, square etch pits form at the surface; the pit density increases while the pits open with an horizontal velocity of 15 nm/min and a vertical velocity of 1.5 nm/min. (e) After 17 h of interaction the pits are still visible. However, a zoom on each pit (f) clearly shows that surface is characterised by microroughness made of protrusions triangle shaped and homogeneously distributed over the surface. (g) After 40 h, surface features are characterised by macrosteps 80–100 nm high and microroughness.

The reproducibility of surface evolution was verified carrying out experiments of galena surface dissolution using different mineral grain of our specimen, and also ex-situ experiments of galena surface dissolution. Galena surface features dissolved

in HCl solution at pH = 1, obtained by ex-situ Tapping mode, are shown in Appendix III. In that figure, etch pits covered by protrusion indicate the same surface features measured by in situ AFM and shown in Figure 2.
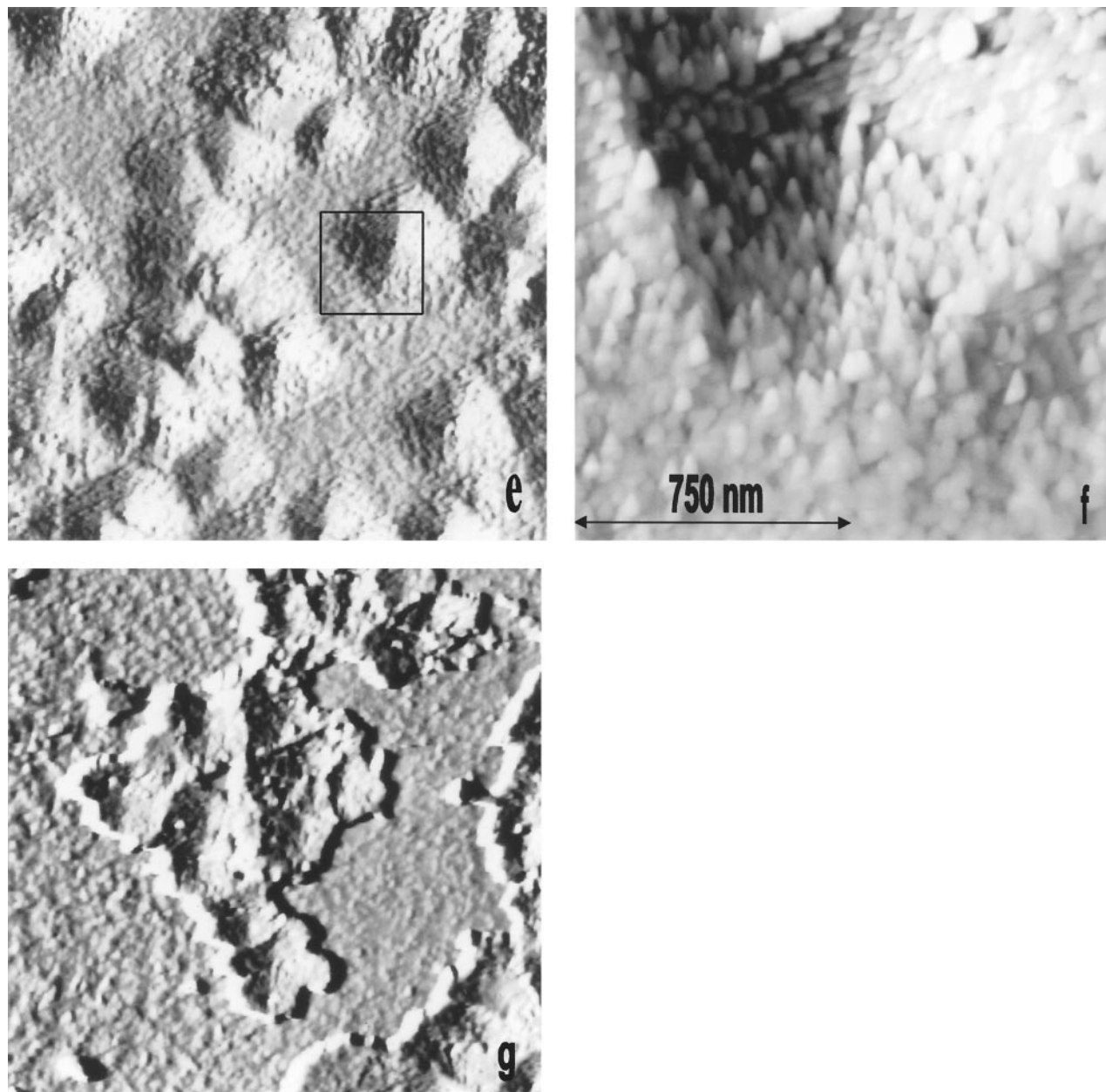
Figure 2. (Continued)

In AFM liquid cell, we investigated dissolution process at condition of pH = 3 (HCl). Dissolution of galena surface at solution pH of 3 proceeds via two different stages as for more acidic condition. Initially, etch pits are 1 to 5 nm deep and cover a large part of the interacting surface and, after 40 h of interaction, protrusions characterise the observed surface features (Appendix III). Although kinetic behaviour at pH = 3 is very similar to the one observed at pH = 1, protrusions have rounded shape. This is probably determined by the lower hydrogen ion activity that rules sulphide speciation in solution. At the condition of pH = 3 solution chemistry indicates the same evolution of rate regime yet observed at pH value of 1. The measured lead concentrations are lower, and dissolution rates decrease independent upon the solution saturation state in both galena and anglesite (these values mean less than 9×10^{-3} and 9×10^{-6}, respectively) by one order of magnitude attaining the final value of 5×10^{-9} mol m^{-2} sec^{-1}. On the other hand, previous AFM study of Whittstock et al. (1996) found clear experimental evidence for protrusion formation at natural galena surface dissolving at solution pH of 4.9 (acetate buffer). Either our data and these literature data indicate that several hours of interaction are needed to observe protrusion formation by AFM. It is probable that molecules of the chemical species composing protrusions are yet present at mineral-water interface at the first instants of interaction, but can not be resolved by AFM because, at this time, they are not attached to the surface as rigid component.

3.3. Mechanistic Implications

Galena dissolution reaction is an intricate process involving both acid-base and redox reaction, and where complexity is added by the high number of electrons involved in the oxidation of sulphur that, in turn, suggests many different potential reaction paths at mineral-water interface. In the geochemical literature, it has been often proposed that galena dissolution rate in acidic and oxidative solutions is controlled by the process of reaction between sulphur and hydrogen to produce sulphide molecules, that are then released from surface and migrate through the interface. In that case, this process should produce surface features controlled by crystallographic properties as indicated by Higgins and Hammers (1996), and result in a clear dependence of the reaction mechanism upon hydrogen concentration as observed by Hsieh and Huang (1989). By contrast, in our experiment, the direct crystallographic control is lost after a short first stage, and dissolution rates evolve indicating a change in the reaction mechanism probably due to a gradual oxidation of galena surface. On the other hand, because of their appearance in AFM images, the nanometric phases that compose protrusions must dissolve slower than galena and should gradually cover the dissolving surface. Because of the size and distribution of pyramidal protrusions and the residence time of solution in our AFM liquid cell (about 20 s) is much shorter than the time of small particle deposition, protrusions are formed during reaction at the interface rather than precipitation from bulk solution. As a consequence of this accumulation of matter at PbS surface, protrusions must influence the diffusion path of the ions at the interface, and produce the observed decrease of dissolution rate. Therefore, our data indicate that the slow intermediate step limiting the rate of the overall reaction is represented by the reaction of protrusion dissolution, and that the thickness of 'protrusion layer' plays a role in the process of dissolution.

When protrusions appear in AFM images, the amount of matter coating the surface allows the complete inhibition of square pitting process, while dissolution is ever active as shown by both solution chemistry and microtopography. We can not derive from our data the absolute velocities of protrusion formation and dissolution, but we can roughly estimate the difference between these two velocities as the amount of matter accumulated at a given time at surface as protrusions. We calculated this value by accounting for the experimental conditions and assuming that protrusions are 3 nm high, cover homogeneously the surface and have a molar volume that approximates the one of galena. This amount increases during the interaction and, at the beginning of square pitting inhibition (Fig. 1e), means $1 \pm 0.5 \times 10^{-9}$ mol representing less than 1% with respect to the total amount of galena that has been dissolved (1×10^{-6} mol) after 17 h. On the other hand, since protrusions accumulate only <1% of total dissolved galena, ΣS released during the overall reaction of galena dissolution should approximate Pb in accord with solution data of Hsieh and Huang (1989). As the dissolution rates tend to a constant value, we can predict that the thickness of the protrusion layer will be constant when the velocity of protrusion formation approximates the velocity of protrusion dissolution. In this hypothesis, the evolution of the kinetic regime observed by solution chemistry is a transitory stage where the continuous increase in the thickness of protrusions influences the interfacial reaction path of the chemical species participating to the dissolution process.

According to different XPS investigations on galena surfaces reacted in acidic and oxidative solutions representative of natural conditions, the microscopic secondary products can correspond to sulphate, lead hydroxides, lead oxides and lead-deficient galena surface (Fornasiero et al., 1994; Kim et al., 1995) while ECSTM indicates that native sulphur islands can be formed and redissolved depending upon the applied electrochemical potential (Higgins and Hammers, 1995). Assuming that surface thermodynamics can be roughly approximated by molar thermodynamics of solution chemistry, we can associate solution chemistry to surface speciation data in the literature to predict the chemical composition of protrusions. Accounting for our conditions, we predicted the precipitation of sulphur and sulphate, whereas lead oxide and lead hydroxides depend upon pH value and should not form under acidic conditions. Lead sulphate, however, is significantly more soluble than galena and should not accumulate at the surface as protrusions. On the other hand, in our experiment, protrusion formation is not linked to the solution saturation state in lead sulphate. We argued this, firstly because solutions circulating in our flow through system are strongly undersaturated in this phase, and secondly because the minimum undersaturation conditions are attained at the start of the experiment whereas the saturation degree decreases during the evolution to the microroughness state. Therefore, native sulphur, a sparingly soluble phase but able to slowly react with oxygen to produce sulphate, should form during the dissolution of galena surface in acidic and oxidative conditions (Garrels and Christ, 1965; Pourbaix and Pourbaix, 1992), and limit the rate of the overall reaction.

During the slow process of sulphur oxidation to sulphate, several thermodynamically unstable species can be kinetically favoured, namely polysulphides, S_n^{-2} n > 2, and sulfoxy anions, $S_2O_3^{2-}$, SO^{2-}, etc. These species have short lifetimes and are sensitive to the experimental conditions (Nowak and Laajalehto, 2000). Since the slow accumulation of sulphur at surface produces a change in both surface stoichiometry and diffusion processes at interface, the observed surface evolution should influence the route of oxidation reaction of sulphur to sulphate. Thus, assuming that the kinetics of formation of the unstable species depend upon the actual state of the surface, the observed evolution in surface microtopography should correspond to a change in the respective amounts of polysulphides and sulfoxy anions produced by surface dissolution at a given time. Unfortunately, we were not able to verify this hypothesis by measuring the chemical speciation of sulphur in the solution, however, this can be done in future works by high sensitive analytical techniques.

Considerations on galena surface charge can lead to a full mechanistic explanation of evolving galena surface. The value of pH isoelectric point ($pH_{i.e.p.}$) for PbS has been measured by electrokinetic measurements to be 1.4 (Bebie et al., 1998). When solution pH has values below $pH_{i.e.p.}$, PbS surface has positive charge allowing fast release of positive lead ions and slow release of sulphur. In our experimental conditions, according to the pristine value of $pH_{i.e.p.}$, some sulphur is then concentrated at the mineral-water interface, perhaps to the point that condition of local supersaturation in sulphur is reached. In

such a way, microscopic processes of dissolution in far from equilibrium conditions could locally follow thermodynamic phase diagrams and, at a given time, reach chemical steady state at the interface. However, evolution of both dissolution rates and galena surface at constant solution pH suggests a deviation of $pH_{i.e.p}$ from pristine value, as indicated by measurements of oxidising pyrite surface where chemisorbed oxygen produces a shift in $pH_{i.e.p.}$ of several unit of pH (Fornasiero et al., 1991). In our experiment, when surface terminates with sulphur atoms and not with sulphides, the loss of negative electric charge associated to sulphide surface sites produces an increase in positive surface charge of oxidising galena and, consequently, a gradual shift from pristine $pH_{i.e.p.}$ to higher $pH_{i.e.p.}$ Thereby, protrusion formation probably imply that the amount of hydrogen ions bonded to the surface decreases during the interaction because of an increase of positive charge and consequent electrostatic repulsion. On the other hand, surface behaviour can be tentatively explained in terms of stoichiometry of crystallographic surfaces. Since (111) crystallographic face is homoatomic while (001) and (110) have a Pb/S ratio of 1, surface charge can be theoretically changed by an increase in the amount of (111) microscopic sulphur surfaces. Such an increase in (111) microfacets, that corresponds also to lower atomic density at surface, is coherent with both shape and distribution of protrusions observed in Figure 2 and is then a possible reaction path for sulphur bonding to the oxidising PbS surface.

In conclusion, we propose that protrusions formation inhibits the direct crystallographic control upon surface features and constitutes a surface microscopic reservoir. This rules the rate of matter exchange between galena and oxygen-saturated solution in Earth surface environments. Since at the constant pH condition of the experiment both reaction rate and surface features significantly change, the mechanistic dependence of galena dissolution with respect to hydrogen concentration changes during the reaction. Therefore, we believe that surface evolution must be taken in account in further mechanistic investigations on galena surface dissolution in acidic and oxidative conditions.

4. SUMMARY AND CONCLUSIONS

Liquid cell AFM and solution chemistry techniques have been coupled performing an in situ investigation that illustrates galena dissolution reaction at different scales.

- During 45 h of interaction with acidic and oxidative solutions at pH = 1 in a flow through AFM liquid cell, galena surface evolves via two different stages. In the short first stage, the microtopography is related to the symmetry of galena and square etch pits form over a part of the surface. Whereas in a second stage pyramidal protrusions cover the surface and nucleation and growth of square pits is stopped. During interaction with oxidative solutions at pH value of 3, galena surface behaviour is the same but protrusions have a rounded shape.

- Kinetic rates, measured by lead concentration in solution, decrease by more than one order of magnitude during the experiments indicating that protrusion accumulation is associated to a decrease of the surface reactivity and a change in the reaction mechanism.

- Based on their appearance in AFM images, protrusions are constituted by slowly soluble phases. We interpreted that the reaction of protrusion dissolution limits the overall dissolution rate and predicted that, at least for our low pH experimental conditions, protrusions are formed by native sulphur.

- Finally, AFM investigation reveals a microscopic surface reservoir that plays a fundamental role in the process of galena dissolution.

Associate editor: J. D. Rimstidt

REFERENCES

Anbeek C. (1992) Surface roughness of minerals and implications for dissolution studies. *Geochim. Cosmochim. Acta* **56,** 1461–1469.

Bebie J., Schoonen M. A. A., Fuhrmann M. at Strongin D. R. (1998) Surface charge development on transition metal sulfides: An electrokinetic study. *Geochim. Cosmochim. Acta* **64,** 633–642.

Eggleston C. M. (1996) Initial oxidation of sulfide sites on a galena surface: Experimental confirmation of an ab-initio calculation. *Geochim. Cosmochim. Acta* **61,** 657–660.

Eggleston C. M. and Hochella M. F. Jr. (1991) Scanning tunneling microscopy of galena (100) surface oxidation and sorption of aqueous gold. *Science* **254,** 983–986.

Fornasiero D., Eijt V., and Ralston J. (1991) An electrokinetic study of pyrite oxidation. *Coll. Surf.* **62,** 63–73.

Fornasiero D., Fengsheng L., Ralston J., and Smart R. (1994) Oxidation of galena surfaces. I. X-Ray photoelectron spectroscopy and dissolution kinetic studies. *J. Colloid Interf. Sci.* **164,** 333–344.

Garrels R. M. and Christ C. L. (1965) Solutions minerals and equilibria. Harper and Rows.

Higgins R. S. and Hamers R. J. (1995) Spatially-resolved electrochemistry of the lead sulfide (galena) (001) surface by electrochemical scanning tunnelling microscopy. *Surf. Sci.* **324,** 263–281.

Higgins R. S. and Hamers R. J. (1996) Chemical dissolution of the galena (001) surface observed using electrochemical scanning tunnelling microscopy. *Geochim. Cosmochim. Acta* **60,** 3067–3073.

Hsieh Y. H. and Huang C. P. (1989) The dissolution of $PbS_{(s)}$ in dilute aqueous solutions. *J. Coll. Int. Sci.* **131,** 537–549.

Jaycock M. J. and Parfitt G. D. (1981) Chemistry of interfaces. Ellis Horwood Publ.

Kim B. S., Hayes R. A., Prestidge C. A., Ralston J., and Smart R. St.C. (1994) Scanning tunnelling microscopy studies of galena: The mechanism of oxidation in air. *Appl. Surf. Sci.* **78,** 385–397.

Kim B., Hayes R. A., Prestidge C. A., Ralston J., and Smart R. St .C. (1995) Scannelling tunnelling microscopy studies of galena: The mechanism of oxidation in aqueous solution. *Langmuir.* **11,** 2554–2562.

Land A. T., Martin T. L., Potapenko S., Palmore G. T., and De Yoreo J. J. (1999) Recovery of surfaces from impurity poisoning during crystal growth. *Nature* **399,** 442–445.

Lasaga A. (1998) Kinetic theory in the Earth Sciences. Princeton Univ. Press.

Nesbitt H. W. and Muir I. J. (1994) X-ray photoelectron spectroscopic study of a pristine pyrite surface reacted with water vapour and air. *Geochim. Cosmochim. Acta* **58,** 4667–4679.

Nesbitt H. W., Muir I. J., and Pratt A. R. (1995) Oxidation of arsenopyrite by air and air-saturated, distilled water, and implications for mechanism of oxidation. *Geochim. Cosmochim. Acta* **59,** 1773–1786.

Nowak P. and Laajalehto K. (2000). Oxidation at galena surface—an XPS study of the formation of sulfoxy species. *Appl. Surf. Sci.* **157,** 101–111.

Pourbaix M. and Pourbaix L. (1992) Potential-pH equilibrium diagrams for the sistems S-H2O from 25°C to 150°C: Influence of access of oxygen in sulfide solutions. *Geochim. Cosmochim. Acta* **56,** 3157–3178.

Reeder R. J. (1991) Surfaces make a difference. *Nature* **353,** 797–798.

Singer P. C. and Stumm W. (1970) Acid mine drainage: The rate limiting step. *Science* **167,** 1121–1123.

Tossel J. A. and Vaughan D. J. (1987) Electronic structure and the chemical reactivity of the surface of galena. *Can. Min.* **25,** 381–392.

Wieland E., Wherli B., and Stumm W. (1988) The coordination chemistry of weathering: III. A generalisation on the dissolution rates of minerals. *Geochim. Cosmochim. Acta* **52,** 1969–1981.

APPENDIX I

| Time (h)	Pb^{2+} mol/l	Saturation state PbS	ΔG KJ mol^{-1} $PbS + H^+ \leftrightarrow$ $Pb^{2+} + HS^-$	Saturation state $PbSO_4$	Dissolution rate mol m^{-2}sec^{-1}
4	5.6×10^{-6}	2×10^{-4}	−21	2×10^{-3}	1.1×10^{-6}
8	4.4×10^{-6}	1×10^{-4}	−22	2×10^{-3}	8.3×10^{-7}
16	8.6×10^{-7}	4×10^{-6}	−29	5×10^{-5}	1.6×10^{-7}
17	7.3×10^{-7}	3×10^{-6}	−30	3×10^{-5}	1.4×10^{-7}
18	7.4×10^{-7}	3×10^{-6}	−30	3×10^{-5}	1.4×10^{-7}
20.5	7.4×10^{-7}	3×10^{-6}	−30	3×10^{-5}	1.4×10^{-7}
22.5	4.8×10^{-7}	1×10^{-6}	−32	1×10^{-5}	9.0×10^{-8}
23.5	5.2×10^{-7}	2×10^{-6}	−32	2×10^{-5}	9.8×10^{-8}
24	5.0×10^{-7}	1×10^{-6}	−32	2×10^{-5}	9.4×10^{-8}
43	2.5×10^{-7}	4×10^{-7}	−35	4×10^{-6}	4.8×10^{-8}
44	2.4×10^{-7}	3×10^{-7}	−35	4×10^{-6}	4.5×10^{-8}

Dissolution of galena in acidic oxidative conditions at pH = 1 (HC1): data of lead concentration in the solution circulating into the AFM liquid cell, estimated saturation state in galena and anglesite, and estimated ΔG (KJ mol^{-1}) with respect to the reaction of galena dissolution ($PbS + H^+ \leftrightarrow Pb^{2+} + HS^-$, $K_s = 10^{-12.75 \pm 0.05}$). Dissolution rate is calculated according to Eqn. 1 (see text for explanation).

APPENDIX II

Time (min)	Width (nm)	Depth (nm)	Time (min)	Width (nm)	Depth (nm)
28	100		38	260	
28	120		38	250	
28	150		38	280	
28	300		38	450	
28	700	25	38	890	45
28	150		38	290	
28	170		38	320	
28	900	25	38	1100	40
28	200		38	340	
28	250		38	400	
28	300		38	430	
28	400	15	38	550	30
28	600	25	38	730	45

DI software measurements of etch pits size in Figure 2c and d. The initial size of pits is influenced by cleavage, the error in measurements is 5%. The mean value for horizontal growth of pits is 15 nm/min. The velocity of vertical growth was estimated to be 1.5 nm/min considering for measurements only largest pits. Note that pit growth is inhibited after some hours of interaction by protrusion formation as shown in Fig. 2e,f,g.

APPENDIX III
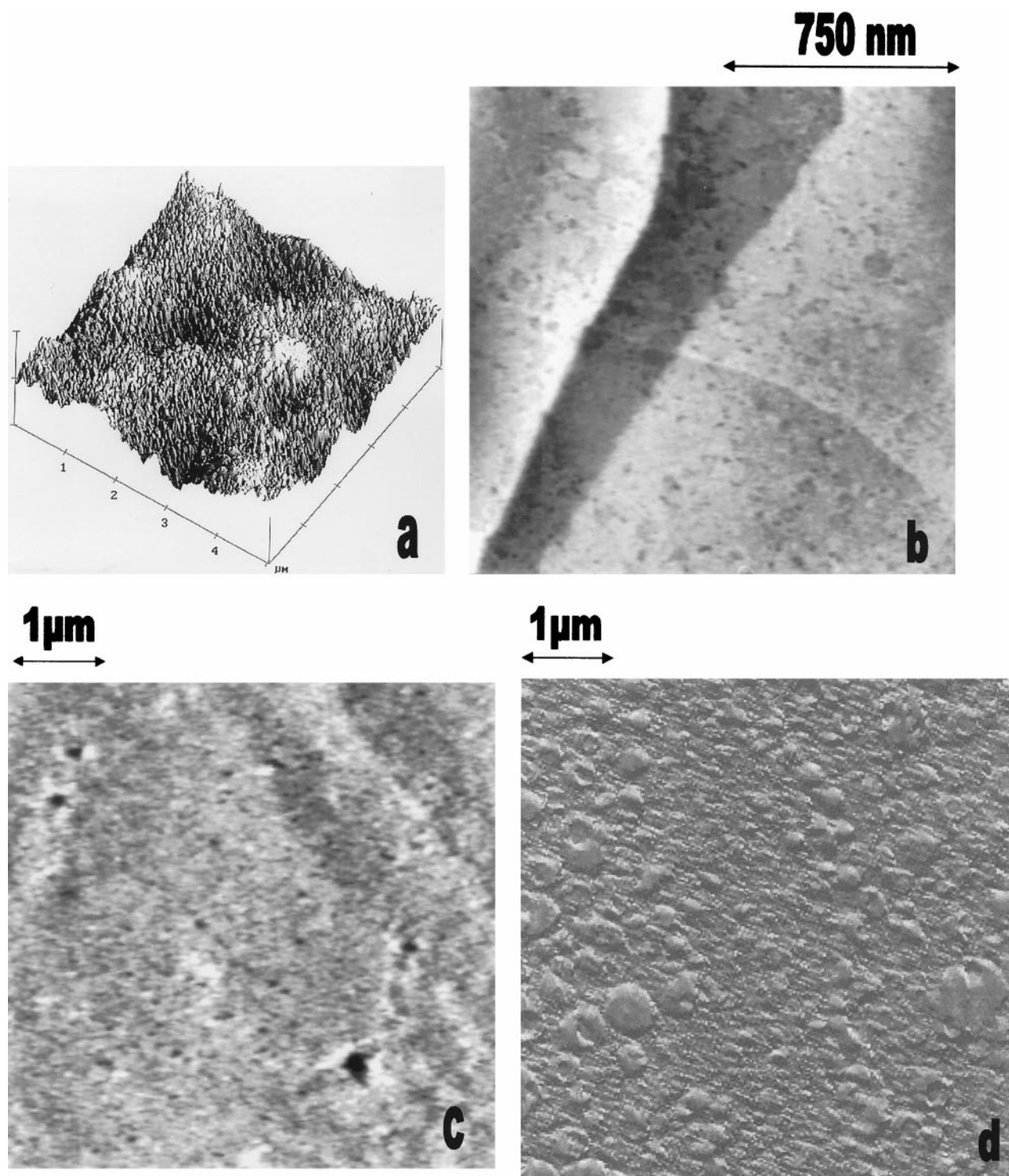
Reproducibility of surface evolution process at pH = 1 and surface dissolution at pH = 3. b), c) and d) were taken with the same experimental method of Figure 2, while a) was taken in ex-situ Tapping mode (scan rate of 0.5 Hz) and is presented in topographic mode, the vertical scale is exaggerated. To carry out data presented in a), galena grain was dissolved in HCl solution (pH = 1) using simple batch reactor and, after 24 hours, separated from solution, carefully dried under vacuum, and then imaged by AFM. In the 5×5 μm image shown in a), surface features are characterised by etch pits 50 nm depth and protrusions 2–5 nm high covering all the surface. Interacting solution was undersaturated in both galena and anglesite (saturation state is 5×10^{-4} and 5×10^{-3}, respectively). b) galena surface dissolution at pH = 3 after 10 min of interaction is characterised by the formation of etch pits 1–2 nm deep, macrosteps are due to cleavage. c) imaging the same surface of b) at larger scale after 20 h we found protrusion formation and, after 40 h of interaction, protrusions 5 nm high are clearly formed but show rounded shape c). Experimental conditions are total surface area $A = 5 \times 10^{-5}$ m^{-2}, solution saturation state in both galena and anglesite less than 9×10^{-3} and 9×10^{-6}, respectively, and rate regime evolved during interaction as observed for the condition pH = 1 (see text for explanation). The results shown in this Appendix indicate that surface behaviour of our galena specimen does not depend upon the particular grain under investigation. However, the value of solution pH could influence protrusion shape.